Challenge Journal of Structural Mechanics

Research Article

Numerical investigation on damage performance of a reinforced concrete structure subjected to machine loads

Memduh Karalar [a,*], Murat Çavuşli [a]

[a] *Department of Civil Engineering, Zonguldak Bülent Ecevit University, İncivez, 67100 Zonguldak, Turkey*

ABSTRACT

Investigation of carrying capacity performance of reinforced concrete (RC) structures is very important for structural engineering. In this study, it is aimed to examine the nonlinear carrying capacity performance of an RC laboratory structure by using three dimensional (3D) modelling approach. For this purpose, Zonguldak Bulent Ecevit University Laboratory Structure is selected and it is modeled as three dimensional by utilizing IDECAD static software. After modelling all beams, columns and floors according to 2018 Turkish earthquake code, concrete classes are determined for all bearing elements and specified concrete classes are defined for all elements of 3D model. Then, structure is analyzed for empty situation (Case 1) and structural performance of building is analyzed to this situation. In the past, a flat of this RC structure has been exposed to strong machine loads. For this reason, a machine which is fixed on the floor is placed in the 3D model and RC structure is analyzed considering nonstructural machine element loads (Case 2). According to analysis results, Case 1 is compared with Case 2 and it is clearly seen that nonstructural machine loads effect nonlinear carrying capacity performance of RC buildings.

ARTICLE INFO

Article history:
Received 19 February 2020
Revised 16 March 2020
Accepted 15 April 2020

Keywords:
Carrying capacity
Damage performance
Three dimensional modelling
Reinforced concrete building

1. Introduction

In the recent years, reinforced concrete (RC) buildings have been frequently used in many world countries for many purposes. Concrete has tremendous compressive strength. Moreover, steel has tremendous tension strength. In the past, a very important idea was suggested about combination of concrete and steel materials. RC buildings have been revealed with this idea that combined concrete and steel. Any defect in concrete or steel element affects all of the structures. The adherence between these materials improves properties of RC elements. The first defect was related with damages in RC buildings that have the weak concrete materials. The importance of studies, researches and prevention about carrying capacity of the RC structures have risen after destructive earthquakes in the world especially in recent years. Demartino et al. (2017) examined an experimental and numerical study about the damage behavior of circular RC columns subjected to impact loading. Numerical study was performed using LS-DYNA software and these numerical results showed a good agreement with the experimental results. Wei et al. (2019) performed an experimental and numerical study about damage performance of reinforced conventional (RC) concrete and ultra-high performance concrete (UHPC) columns subjected important loads. In that study, there are total two different test specimens and these specimens have square and circular cross-section shapes. Moreover, each specimen group includes both RC and UHPC columns. After examined experimental results, numerical simulations were performed to observe residual loading capacity of UHPC column subjected to lateral impacts. Chen et al. (2019) evaluated damage performances of reinforced concrete (RC) columns. In that study, new compression-shear failure mode for RC columns was reported and discussed in detail. A finite element (FE) model was developed by using LS-DYNA. An important equation was proposed to rapidly evaluate the damage situation of the RC columns. Zhao et al.

* *Corresponding author*. Tel.: +90-372-291-2582 ; Fax: +90-372-257-4023 ; E-mail address: memduhkaralar@beun.edu.tr (M. Karalar)
ISSN: 2149-8024 / DOI: https://doi.org/10.20528/cjsmec.2020.03.004

(2020) investigated an experimental and numerical study about steel-concrete (SC) slabs subjected to blast loads. In that study, three small-scale reinforced concrete (RC), single-side- steel-concrete (SSSC) and center steel-concrete (CSC) slabs were tested to acquire the failure modes, mid-span deflection, and dynamic response. 3D numerical models were verified by the experimental tests. According to results, the damaged areas of concrete in SSSC and CSC slabs are larger than RC slab. Biswas et al. (2020) investigated numerical and experimental effects of non-uniform rebar corrosion on damage performance of reinforced concrete (RC) buildings. Damage behavior of RC beams subjected to non-uniform rebar corrosion was examined using three-dimensional (3D) nonlinear finite element (FE) analysis and experimental study. Seven RC beams were tested by using static loads. According to experimental and numerical study results, non-uniform corrosion in the steel bars cause to an important decrease in the load carrying capacity of RC beams. Kumar et al. (2020) performed experimental and numerical study about damage performance of reinforced concrete (RC) slabs subjected to blast loads. The finite element (FE) modelling was performed by using ABAQUS software. According to numerical results, the pressure of blast increase with an increase in the amount of TNT. Mohammed et al. (2020) examine damage performance of reinforced concrete (RC) structures subject to flexural loads. According to results, the damage behaviour of RC systems can be determined with the tensile cracking of the grout and failing of teeth at the joint. Moreover, there are many studies in the literature about damage performance of RC buildings (e.g. Xinchen and Bing (2020), Xian-Liang et al. (2019), Yang et al. (2019), Junsheng et al. (2020), Shuijing et al. (2019), Sulaem and Sudip (2019), Rajib et al. (2020), Li et al. (2020), Tie-shuan et al. (2019), Chen et al. (2019)).

As seen these studies, many investigators have contributed to the literature about nonlinear behaviour of RC buildings. However, effects of machine loads on damage capacity of RC structures have not been examined in the literature. In this study, Zonguldak Bulent Ecevit University laboratory structure is selected for numerical analyses. This structure has a damaged floor at third flat and this floor carries very strong machine loads for a long time. Therefore, examination of this floor is very important for structural engineering. After 3D model of the structure is created according to 2018 Turkish earthquake code, machine loads are applied to this damaged floor and all numerical results are compared with each other.

2. Methodology

In this study, a four story University building frequently exposes very stronger machine loads is examined by using 3D modelling. Because of this RC building carries very serious loads on the floors, examination of damage capacity performance of this structure is very important for the people and structures. First of all, the relievo of the RC building was obtained in detail. Each carrying element is determined in detail and the length information of each carrying element is entered in detail in the AUTOCAD program. Then, information was obtained about the current status of the fittings in the carrying elements using an x-ray device. The 3D model of the building was created with the help of the IDECAD static program. All carrying elements have been carefully entered into the program and the floors have been created in accordance with the project. Finally, core samples were taken from the structure. Considering the historical feature of the building, care was taken not to damage the building too much. Core samples were experimentally tested and their mechanical properties were determined. Total 30 different samples are used to obtained concrete classes of samples. While performing these tests, Turkish TS500 standard was considered and according to test results, average concrete class of these samples is obtained as C20. The material parameters of all carryings are carefully defined in the program. The analyses were first made for the empty status of the building considering 2018 Turkish earthquake code. Then, 30-ton machine load was applied to damaged floor of the structure and 3D model was analyzed taking into account this situation of the structure. According to analysis results, both situations of the structure are compared in detail.

3. Description and 3D Modelling of the RC Building

Zonguldak Bulent Ecevit University Laboratory was constructed in Zonguldak province in 2009. It is located in the University campus. It is a reinforced concrete (RC) building and it has 4 different flats. First and second flats have very heavy machines which are located on the floors and these machines are very critical for civil engineering technology. All flats have coffered slabs and these coffered slabs have very different thicknesses and mechanical properties from each other. These thicknesses are 12 cm, 14 cm, 15 cm, and 18 cm, respectively. Moreover, concrete classes of these slabs are C18, C20 and C22, respectively. Zonguldak Bulent Ecevit University Laboratory building is shown in Fig. 1. Moreover, views of the laboratory building projects are presented for the first floor, second floor, third floor and fourth floor in Fig. 2.

Building has 48 various columns and 88 different beams. Moreover, there are 37 various shear walls in this structure. Height of the first floor is 5 m and height of second, third and fourth floors are 5.2 m, 5.8 m and 4.2 m, respectively. First flat is used for building materials laboratory. Second flat is used for construction technology laboratory and other flats are constructed for office. While creating this structure, one floor of this building collapsed and this floor was rebuilt. This floor is at the third flat of this structure. Then, heavy machines had to be placed on this floor. This structure has been modelled by using 3D modelling approach. While performing modelling, IDECAD static software is used. Firstly, foundation of structure is created according to original project. After columns and beams are modelled, coffered slabs are created in 3D model as seen in Fig. 3. Then, structure is analyzed for empty situation of the building. After that, machine loads are calculated and these loads are applied

to collapsed floor (Fig. 4) and building is analyzed according to this situation. Moreover, fix boundary conditions are defined under the foundation of the building. According to analysis results, both situations of the structure are compared in detail.

4. Three Dimensional Analysis Results

Examination of 3D damage performance of reinforced concrete (RC) buildings is very important for civil engineers. Firstly, x-ray devices were used to determine current situation of the rebars (Fig. 5). Then, the compressive strength of the carrying elements was determined with the Schmidt hammer device. With this device, 15 strokes were applied to each carrying element and concrete classes of these elements are obtained by this device. According to numerical analysis results, empty and full situations of collapsed floor are examined and compared with each other (Tables 1-8). In Tables 1-4, performance analysis results are shown for empty situation of the floor in detail. Moreover, 3D performance results are presented for full situation which there are machine loads on the floor in Tables 5-8. In the numerical results, empty situation of the floor is named as Case 1 and other situation is named as Case 2.

Fig. 1. View of the Laboratory Building.

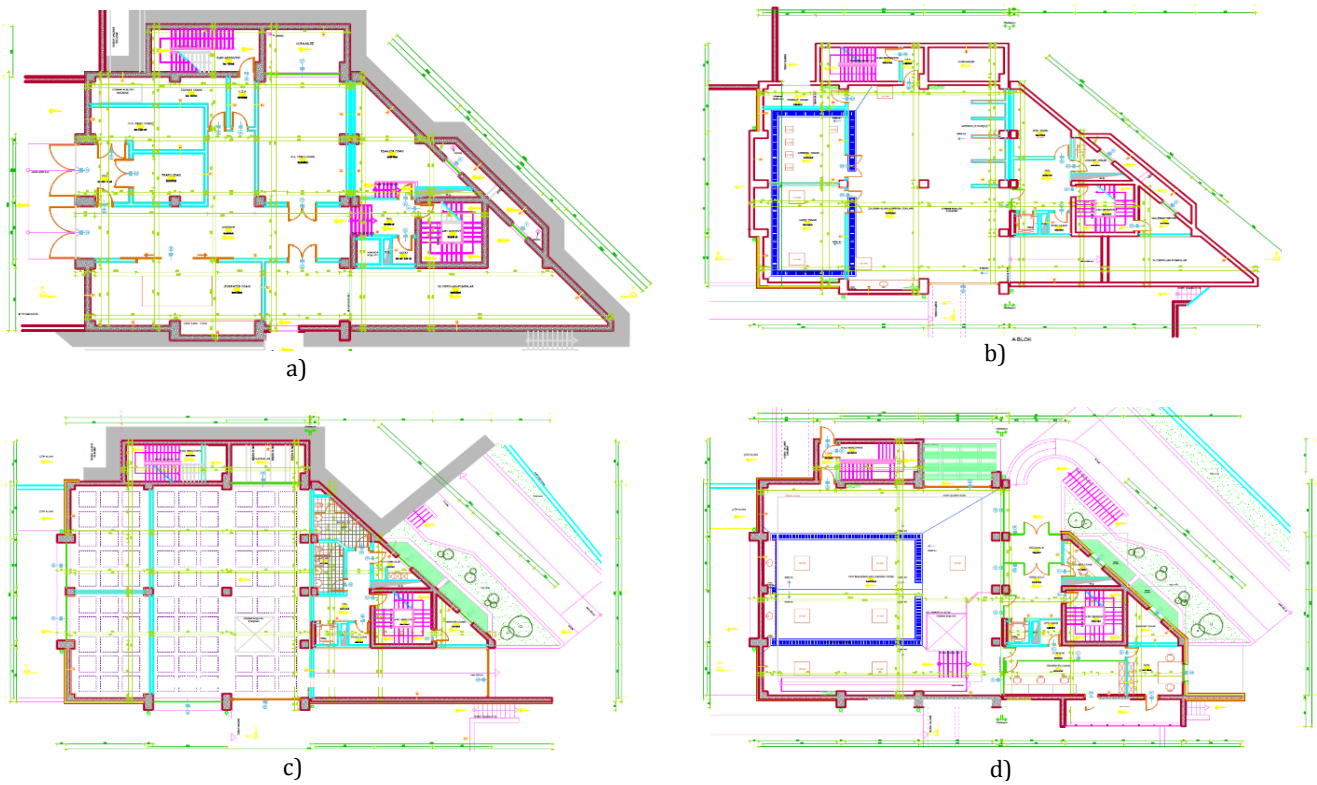

Fig. 1. View of the Laboratory Building projects: a) First floor; b) Second floor; c) Third floor; d) Fourth floor.

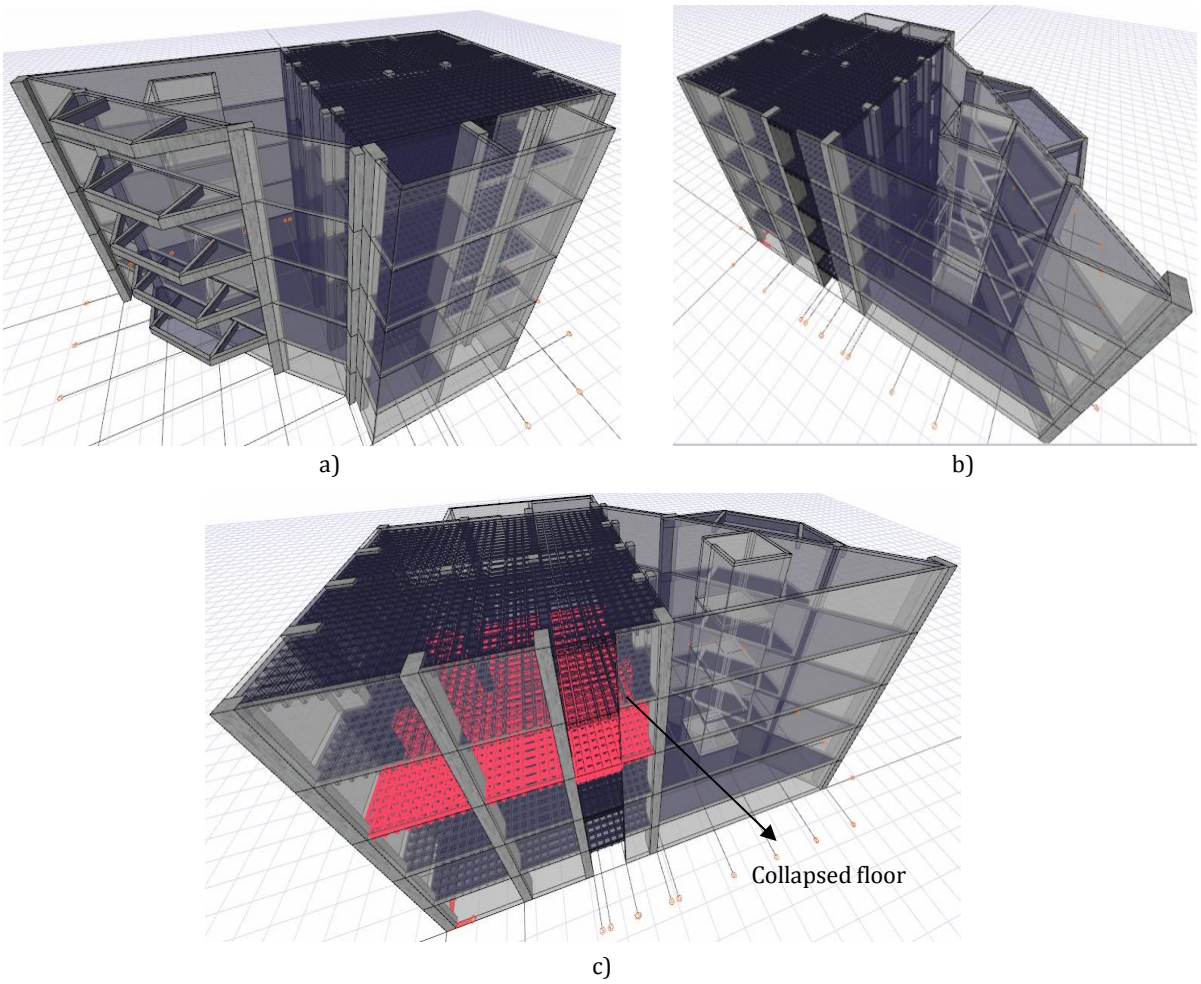

Fig. 3. 3D model of Laboratory Building.

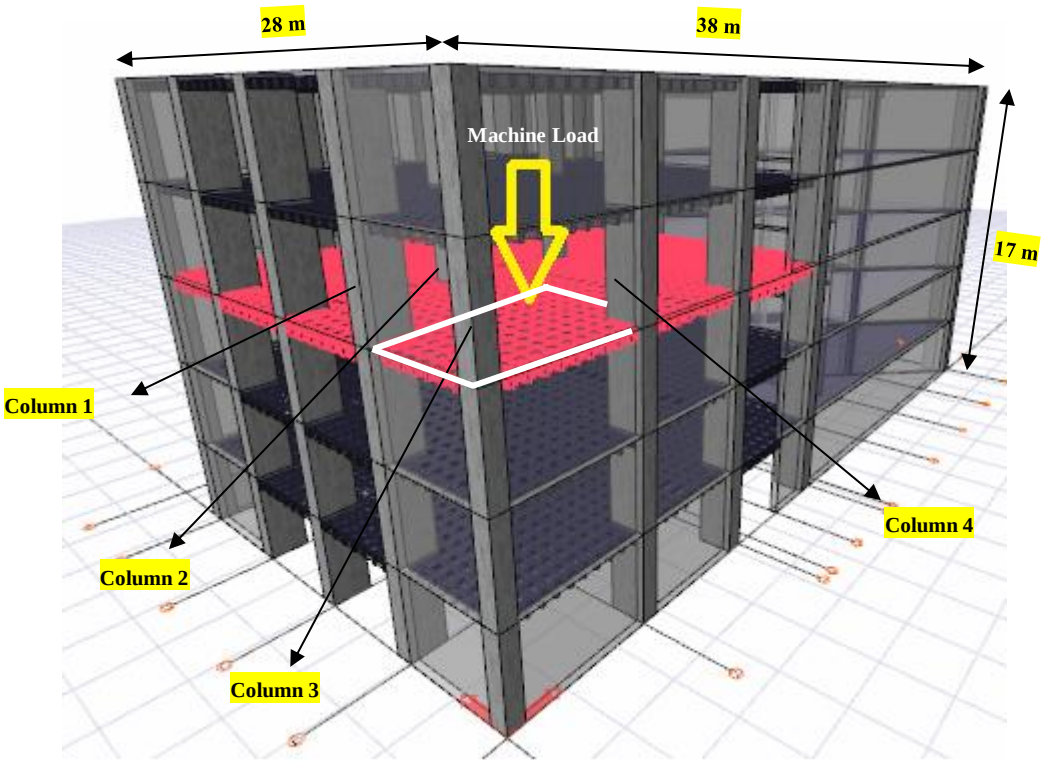

Fig. 4. Machine load on collapsed floor.

Fig. 5. Examination of carrying elements with X-ray device.

In Table 1, numerical results of column 1 (Ni, V2i, V3i, M2i, M3i, Nj, V2j, V3j, M2j, M3j) are shown for Case 1 in detail. Maximum loads are marked in bold. In addition, these loads are presented for 8 different combinations of 2019 Turkish Earthquake Code. According to Table 1, maximum normal load (Ni) is -11.90 kN for G+Q+EY2 combination and maximum shear load (Vi) is 5.24 kN for G+Q+EX2 combination. In addition, maximum moment load (Mi) is 5.71 kNm for G+Q+EY1 combination (Table 1). Maximum normal load (Nj) for j direction of column 1 is 12.42 kN for G+Q-EY1 combination and maximum shear load (Vj) is 4.69 kN. Besides, maximum moment load (Mj) is 7.81 kNm as seen from Table 1.

In Table 2, three dimensional numerical results (Ni, V2i, V3i, M2i, M3i, Nj, V2j, V3j, M2j, M3j) for column 2 are presented for Case 1. -27.82 kN maximum normal load (Ni) is obtained for G+Q+EY1 combination. Moreover, -4.21 kN maximum shear load (Vi) is obtained for G+Q+EY1 combination and maximum moment load (Mi) is 13.72 kNm for G+Q-EY1 combination. When compared Tables 1 and 2, column 2 has more normal load and moment value than column 1 as seen from Tables 1 and 2. Maximum normal load (Nj) for j direction of column 2 is -12.16 kN. This load value is very close to column 1. Maximum shear load (Vj) is -3.31 kN and maximum moment load (Mj) is -3.40 kNm for G+Q+EY1 combination (Table 2).

Table 1. Numerical analysis results of Column 1 for Case 1.

Load	Ni	V2i	V3i	M2i	M3i	Nj	V2j	V3j	M2j	M3j
Unit		kN		kNm			kN		kNm	
G+Q+EX1	-11.25	4.74	1.12	2.79	2.77	4.71	1.12	1.03	1.17	**7.81**
G+Q+EX2	-10.60	**5.24**	1.47	3.61	3.14	5.49	2.58	-1.08	1.25	4.91
G+Q+EY1	-11.00	3.28	2.73	3.72	**5.71**	2.20	**4.69**	-3.59	2.39	2.99
G+Q+EY2	**-11.90**	1.13	2.83	1.99	-5.35	8.49	3.42	-1.25	2.21	1.52
G+Q-EX1	-11.25	-1.17	2.57	-1.29	-2.75	11.98	-2.61	2.47	2.36	-4.71
G+Q-EX2	-11.69	-1.67	2.12	-1.01	-2.71	12.39	-2.02	1.39	3.37	-4.79
G+Q-EY1	-5.60	0.29	-2.37	-2.43	-5.09	**12.42**	3.46	0.77	1. 44	-1.70
G+Q-EY2	-4.70	0.44	-2.57	-2.74	2.73	11.67	2.29	3.24	-2.88	2.97

Table 2. Numerical analysis results of Column 2 for Case 1.

Load	Ni	V2i	V3i	M2i	M3i	Nj	V2j	V3j	M2j	M3j
Unit		kN		kNm			kN		kNm	
G+Q+EX1	-12.46	-1.32	2.45	6.69	3.27	-5.97	-1.11	**-3.31**	-2.75	-0.82
G+Q+EX2	-11. 53	1.17	1.15	5.17	3.26	-6.54	-1.18	-1.11	-2.54	-0.23
G+Q+EY1	**-27.82**	**-4.21**	-1.68	3.87	-7.32	**-12.16**	-2.57	-1.29	**-3.40**	-0.64
G+Q+EY2	-21.61	-3.99	-2.51	-4.98	-6.76	-11.19	-2.97	-1.77	-3.09	-0.72
G+Q-EX1	-13.06	-2.71	-2.77	-4.36	-3.69	-4.97	-1.93	-1.63	-1.97	-0.06
G+Q-EX2	-10.84	-2.77	-2.47	-5.19	-4.82	-6.18	-1.44	-1.51	-1.06	-0.59
G+Q-EY1	-12.07	2.81	-1.14	-6.99	**13.72**	-7.83	-0.58	-1.19	-1.34	0.86
G+Q-EY2	-10.37	2.36	-1.67	4.57	4.26	-2.37	-1.96	-1.97	-1.37	-0.47

According to Table 3, numerical results for column 3 (Ni, V2i, V3i, M2i, M3i, Nj, V2j, V3j, M2j, M3j) are shown for Case 1. Maximum loads are marked in bold. In Table 3, maximum normal load (Ni) is -42.84 kN for G+Q+EY1 combination. More normal load value is acquired for column 3, when compared columns 1, 2. Moreover, maximum shear load (Vi) is 5.92 kN for G+Q+EY1 combination and maximum moment load (Mi) is 13.75 kNm for G+Q-EY1 combination. Maximum normal load (Nj) for j direction of column 3 is 1.93 kN. This load value is very less from columns 1 and 2. Maximum shear load (Vj) is -1.99 kN and maximum moment load (Mj) is 1.97 kNm (Table 3). When compared Tables 1, 2 and 3, less moment values are obtained for j direction of column 3.

Table 3. Numerical analysis results of Column 3 for Case 1.

Load	Ni	V2i	V3i	M2i	M3i	Nj	V2j	V3j	M2j	M3j
Unit		kN		kNm			kN		kNm	
G+Q+EX1	-34.01	1.01	1.87	5.97	-2.75	1.52	-1.75	1.45	-1.58	**1.97**
G+Q+EX2	-36.26	1.52	1.85	4.75	3.14	1.57	-1.65	1.53	-1.74	1.85
G+Q+EY1	**-42.84**	-3.55	1.21	1.57	-11.96	1.59	-1.87	-1.26	1.73	1.56
G+Q+EY2	-42.80	-2.74	1.47	1.41	-10.63	**1.93**	-1.21	-1.22	1.65	1.41
G+Q-EX1	-39.71	1.73	-1.57	-4.17	3.93	1.34	-1.19	-1.78	1.58	1.29
G+Q-EX2	-39.67	1.89	-1.96	-4.58	-3.29	1.08	-1.52	-1.89	1.82	1.87
G+Q-EY1	-35.97	**5.92**	-0.63	-3.99	**13.75**	1.82	-1.48	1.55	-1.27	1.89
G+Q-EY2	-35.88	4.28	0.39	-0.85	12.59	1.27	**-1.99**	1.23	-1.89	1.03

In Table 4, numerical results of column 4 (Ni, V2i, V3i, M2i, M3i, Nj, V2j, V3j, M2j, M3j) are shown for Case 1. Maximum loads are marked in bold and these loads are presented for 8 different combinations of 2019 Turkish Earthquake Code. According to Table 4, maximum normal load (Ni) is -38.39 kN for G+Q+EY1 combination. Less normal load value is acquired for column 4, when compared column 3. Moreover, maximum shear load (Vi) is 5.88 kN for G+Q+EY1 combination and maximum moment load (Mi) is 15.87 kNm for G+Q-EY1 combination. Maximum normal load (Nj) for j direction of column 4 is 3.99 kN. This load value is very less from columns 1 and 2. Maximum shear load (Vj) is -1.91 kN and maximum moment load (Mj) is 1.95 kNm (Table 4). When compared Tables 1, 2, 3 and 4, maximum moment value for j direction is obtained for column 4.

Table 4. Numerical analysis results of Column 4 for Case 1.

Load	Ni	V2i	V3i	M2i	M3i	Nj	V2j	V3j	M2j	M3j
Unit		kN		kNm			kN		kNm	
G+Q+EX1	-32.15	2.58	3.78	5.47	4.87	3.52	-1.75	1.52	-1.67	-0.87
G+Q+EX2	-33.58	2.41	2.94	4.95	5.24	3.08	-1.54	1.26	-1.89	-0.85
G+Q+EY1	**-38.39**	-3.39	1.71	2.28	-11.86	3.57	-1.58	1.45	0.57	-1.56
G+Q+EY2	-33.78	-3.85	-1.05	-3.87	-12.17	3.76	-1.79	-1.64	1.60	-1.33
G+Q-EX1	-32.68	1.52	-1.87	-5.08	-5.46	**3.99**	-1.25	-1.52	1.58	-1.58
G+Q-EX2	-33.54	1.22	-1.87	-5.87	-3.67	3.84	-1.05	-1.42	0.97	-1.38
G+Q-EY1	-34.29	**5.88**	-1.97	-1.57	**15.87**	3.75	**-1.91**	1.55	-1.87	**-1.95**
G+Q-EY2	-37.75	4.57	1.78	1.93	10.97	3.88	-1.72	1.26	-0.56	-1.56

According to Table 5, numerical results of column 5 (Ni, V2i, V3i, M2i, M3i, Nj, V2j, V3j, M2j, M3j) are shown for Case 2. In Table 5, maximum normal load (Ni) is -22.97 kN for G+Q+EY2 combination. Moreover, maximum shear load (Vi) is 9.54 kN for G+Q+EX1 combination and maximum moment load (Mi) is 27.69 kNm for G+Q+EX1 combination. Maximum normal load (Nj) for j direction of column 5 is 21.54 kN. Maximum shear load (Vj) is 12.28 kN and maximum moment load (Mj) is 11.59 kNm (Table 5).

In addition, numerical results of column 6 (Ni, V2i, V3i, M2i, M3i, Nj, V2j, V3j, M2j, M3j) are shown in Table 6. According to Table 6, maximum normal load (Ni) is -26.88 kN for G+Q+EY2 combination. Moreover, maximum shear load (Vi) is -8.92 kN for G+Q-EX1 combination and maximum moment load (Mi) is -35.33 kNm for G+Q-EX2 combination. Maximum normal load (Nj) for j direction of column 5 is -14.44 kN. Maximum shear load (Vj) is -4.67 kN and maximum moment load (Mj) is -6.97 kNm (Table 6).

Table 5. Numerical analysis results of Column 1 for Case 2.

Load	Ni	V2i	V3i	M2i	M3i	Nj	V2j	V3j	M2j	M3j
Unit		kN		kNm			kN		kNm	
G+Q+EX1	-13.58	**9.54**	1.63	8.78	**27.69**	10.64	**12.28**	-0.25	-1.58	**11.59**
G+Q+EX2	-13.92	6.87	2.33	9.89	24.54	12.57	5.59	-0.15	-1.97	6.97
G+Q+EY1	-21.05	1.99	5.24	12.62	-3.57	17.78	0.77	-1.68	-0.82	-3.98
G+Q+EY2	**-22.97**	-1.57	6.85	16.48	-5.73	18.85	1.98	-1.48	-2.05	-1.85
G+Q-EX1	-21.52	-5.26	-0.64	-9.04	-22.67	**21.54**	-4.56	-1.88	4.41	-5.57
G+Q-EX2	-21.04	-6.47	-0.67	-10.07	-21.82	20.78	-5.87	-1.70	5.23	-4.80
G+Q-EY1	-16.89	2.88	-4.62	-16.52	4.06	13.90	1.59	0. 06	4.52	3.05
G+Q-EY2	-15.75	1.16	-5.27	-20.24	10.79	12.06	1.03	0.68	4.22	4.87

Table 6. Numerical analysis results of Column 2 for Case 2.

Load	Ni	V2i	V3i	M2i	M3i	Nj	V2j	V3j	M2j	M3j
Unit		kN		kNm			kN		kNm	
G+Q+EX1	-14.25	4.52	5.55	19.52	13.05	-12.98	-3.00	-2.58	-5.87	-6.28
G+Q+EX2	-16.63	4.72	6.56	18.05	20.77	-11.74	-3.65	-4.26	-5.52	**-6.97**
G+Q+EY1	**-26.88**	-6.26	-2.78	-5.24	-33.52	**-14.44**	**-4.67**	-1.64	-1.67	-4.58
G+Q+EY2	-24.57	-4.37	-1.99	-6.54	-32.72	-12.65	2.99	-1.58	-1.60	-5.54
G+Q-EX1	-22.53	-5.16	**-8.92**	-24.65	-31.25	-12.25	-1.57	-1.57	-1.68	2.17
G+Q-EX2	-23.17	-6.88	-7.59	-20.54	**-35.33**	-11.59	-1.88	-1.58	0.15	1.19
G+Q-EY1	-11.19	6.80	-1.22	4.58	22.58	-12.88	1.82	-2.92	-4.65	-1.58
G+Q-EY2	-15.65	1.71	1.27	7.55	10.89	-11.62	0.28	-1.57	-2.74	1.86

According to Table 7, numerical results of column 7 (Ni, V2i, V3i, M2i, M3i, Nj, V2j, V3j, M2j, M3j) are shown for Case 2. In Table 7, maximum normal load (Ni) is -78.99 kN for G+Q+EY2 combination. Moreover, maximum shear load (Vi) is 19.98 kN for G+Q-EY2 combination and maximum moment load (Mi) is -54.88 kNm for G+Q+EY2 combination. Maximum normal load (Nj) for j direction of column 7 is 42.89 kN. Maximum shear load (Vj) is -6.91 kN and maximum moment load (Mj) is 7.58 kNm (Table 7).

In addition, numerical results of column 8 (Ni, V2i, V3i, M2i, M3i, Nj, V2j, V3j, M2j, M3j) are shown in Table 8. According to Table 8, maximum normal load (Ni) is -77.78 kN for G+Q+EY1 combination. Moreover, maximum shear load (Vi) is 12.88 kN for G+Q-EY1 combination and maximum moment load (Mi) is -52.91 kNm for G+Q+EY1 combination. Maximum normal load (Nj) for j direction of column 8 is 54.78 kN. Maximum shear load (Vj) is 6.92 kN and maximum moment load (Mj) is 5.92 kNm (Table 8).

Table 7. Numerical analysis results of Column 3 for Case 2.

Load	Ni	V2i	V3i	M2i	M3i	Nj	V2j	V3j	M2j	M3j
Unit		kN		kNm			kN		kNm	
G+Q+EX1	-70.28	-1.57	9.85	36.25	-24.54	41.54	-4.85	5.28	6.37	5.58
G+Q+EX2	-70.85	-2.58	9.74	36.64	-26.42	41.24	-4.80	5.52	**7.58**	6.45
G+Q+EY1	-73.84	-15.97	-4.25	7.58	-52.27	42.67	-3.56	3.19	6.57	6.68
G+Q+EY2	**-78.99**	-16.52	3.64	8.73	**-54.88**	**42.89**	-3.66	2.10	4.88	6.99
G+Q-EX1	-73.95	3.27	-4.55	-37.34	26.89	39.52	-3.85	**-6.91**	2.28	3.82
G+Q-EX2	-72.57	3.44	-9.41	-37.48	27.92	39.54	-4.57	-5.58	2.48	-2.58
G+Q-EY1	-66.08	14.66	-4.58	-6.59	48.11	38.59	-4.12	-3.77	4.08	1.71
G+Q-EY2	-62.57	**19.98**	-4.87	-8.85	50.57	38.97	-4.26	-2.52	4.14	-1.29

Table 8. Numerical analysis results of Column 4 for Case 2.

Load	Ni	V2i	V3i	M2i	M3i	Nj	V2j	V3j	M2j	M3j
Unit		kN		kNm			kN		kNm	
G+Q+EX1	-72.28	4.88	9.47	34.93	18.25	44.22	-1.67	**6.92**	5.38	2.52
G+Q+EX2	-72.68	5.54	9.85	34.26	24.78	44.07	-2.58	5.23	**5.92**	2.25
G+Q+EY1	**-77.78**	-9.46	-1.29	8.38	**-52.91**	**54.78**	2.77	2.67	4.47	2.29
G+Q+EY2	-76.62	-9.67	-1.97	-8.18	-46.28	44.89	1.20	2.56	5.42	2.71
G+Q-EX1	-73.05	-3.20	-9.97	-36.55	-36.44	43.55	-2.11	-4.29	2.50	5.85
G+Q-EX2	-74.64	-3.58	-9.48	-35.22	-33.56	43.52	-2.13	-4.71	1.77	5.29
G+Q-EY1	-69.17	**12.88**	-1.26	-8.20	45.69	41.17	-6.17	2.58	3.70	5.33
G+Q-EY2	-69.28	10.45	-1.58	8.84	40.33	41.69	-4.59	2.93	2.59	5.19

5. Conclusions

In this study, it is aimed to understand and show how important the non-structural elements are for the bearing capacities of the structures. For this purpose, in this study, Zonguldak Bulent Ecevit University laboratory building was selected for 3D modeling. After the building was modeled, machine load was given to the building and it was analyzed for two different situations (Cases 1and 2). Empty floor is named as Case 1 and floor with machine loads is named as Case 2 in this study. Considering the results of the analysis, it will be useful to consider the below suggestions:

- As seen these numerical results, nonstructural machines clearly affect the carrying loads (Ni, V2i, V3i, M2i, M3i, Nj, V2j, V3j, M2j, M3j) on carrying elements of the reinforced concrete buildings.
- When compared Cases 1 and 2, more normal loads are obtained for Case 2.
- Buildings with significant machine loads, such as laboratories, should be modelled taking into account these machine loads.
- It is obviously suggested that all machines on the damaged floor of the building must be removed. Because machine loads significantly increase the loads on all carrying elements.

References

Biswas RC, Iwanami M, Chijiwa N, Uno K (2020). Effect of non-uniform rebar corrosion on structural performance of RC structures: A numerical and experimental investigation. *Construction and Building Materials*, 230, 116908.

Chen L, Hu Y, Ren H, Xiang H, Zhai C, Fang Q (2019). Performances of the RC column under close-in explosion induced by the double-end-initiation explosive cylinder. *International Journal of Impact Engineering*, 132, 103326.

Chen X, Xinzheng L, Xuchuan L (2019). Damage assessment of shear wall components for RC frame–shear wall buildings using story curvature as engineering demand parameter. *Engineering Structures*, 189, 77-88.

Demartino C, Wu J, Xiao Y (2017). Experimental and numerical study on the behavior of circular RC columns under impact loading. *Procedia Engineering*, 199, 2457-2462.

Junsheng S, Zhongxian L, Junjie W, Rajesh PD (2020). Numerical simulation and damage analysis of RC bridge piers reinforced with varying yield strength steel reinforcement. *Soil Dynamics and Earthquake Engineering*, 130, 106007.

Kumar V, Kartik KV, Iqbal MA (2020). Experimental and numerical investigation of reinforced concrete slabs under blast loading. *Engineering Structures*, 206, 110125.

Li Y, Yin S-p, Chen W-j (2020). Seismic behavior of corrosion-damaged RC columns strengthened with TRC under a chloride environment. *Construction and Building Materials*, 201, 736-745.

Mohammed AA, Manalo AC, Maranan GB, Muttashar M, Zhuge Y, Vijay PV, Pettigrew J (2020). Effectiveness of a novel composite jacket in repairing damaged reinforced concrete structures subject to flexural loads. *Composite Structures*, 233, 111634.

Rajib KB, Mitsuyasu I, Nobuhiro C, Kunihiko U (2020). Effect of non-uniform rebar corrosion on structural performance of RC structures: A numerical and experimental investigation. *Construction and Building Materials*, 230, 116908.

Shuijing X, Longhe X, Zhongxian L (2019). Seismic performance and damage analysis of RC frame–core tube building with self-centering braces. *Soil Dynamics and Earthquake Engineering*, 120, 146-157.

Sulaem ML, Sudip T (2019). A study on the performance of damaged RC members repaired using ultra-fine slag based geopolymer mortar. *Construction and Building Materials*, 217, 216-225.

Tie-shuan Z, Ming-yang W, Cheng-yu Y, Tao Z, Chao G (2019). Experimental investigation on dynamic response and damage models of circular RC columns subjected to underwater explosions. *Defence Technology*, In Press.

Wei J, Li J, Wu C (2019). An experimental and numerical study of reinforced conventional concrete and ultra-high performance concrete columns under lateral impact loads. *Engineering Structures*, 201, 109822.

Xian-Liang R, Shan-Suo Z, Yi-Xin Z, Xiao-Yu Z, Li-Guo D (2019). Experimental study on the seismic behavior of RC shear walls after freeze-thaw damage. *Engineering Structures*, 206, 110101.

Xinchen Z, Bing L (2020). Damage characteristics and assessment of corroded RC beam-column joint under cyclic loading based on acoustic emission monitoring. *Engineering Structures*, 205, 110090.

Yang Z, Yanping Z, Marlyn Y, Dongliang M, Xudong S, Qi D, Genda C (2019). Flexural behaviors and capacity prediction on damaged reinforcement concrete (RC) bridge deck strengthened by ultra-high performance concrete (UHPC) layer. *Construction and Building Materials*, 215, 347-359.

Zhao C, Lu X, Wang Q, Gautam A, Wang J, Mo YL (2019). Experimental and numerical investigation of steel-concrete (SC) slabs under contact blast loading. *Engineering Structures*, 196, 109337.